Science Advances
AAAS

advances.sciencemag.org/cgi/content/full/6/12/eaaz1096/DC1

Supplementary Materials for

Mediterranean radiocarbon offsets and calendar dates for prehistory

Sturt W. Manning*, Bernd Kromer, Mauro Cremaschi, Michael W. Dee, Ronny Friedrich, Carol Griggs, Carla S. Hadden

*Corresponding author. Email: sm456@cornell.edu

Published 18 March 2020, *Sci. Adv.* **6**, eaaz1096 (2020)
DOI: 10.1126/sciadv.aaz1096

This PDF file includes:

Supplementary Materials and Methods

Intra-annual offsets in ^{14}C measurements

Observations of the seasonal (intra-annual) cycle of atmospheric ^{14}C exist only for the past 60 years (22, 60–74), when bomb radiocarbon and fossil fuel (^{14}C-free) emissions dominate the seasonal cycle. However, time-varying stratospheric-tropospheric exchange, biospheric carbon fluxes, and cross-equator exchange is estimated to contribute ~3‰ to the seasonal cycle of the northern hemisphere, with a minimum in March and a maximum in September. For example, the ^{14}C values for *Picea abies* tree-rings from near the Schauinsland station (southern Germany) "closely match the summer values of the air samples averaged over the months May to August" (*64*), reflecting the later spring through summer growing season for this tree. The IntCal curve, through the IntCal13 iteration (*4*), primarily reflects this same later spring through summer record (thus peak intra-annual ^{14}C levels (ref. 65 at p.1279)), given the typical tree growth period in central to northern Europe and in temperate to cooler northern North America. In contrast, radiocarbon dating of plant material with growth periods which reflect different parts of the annual ^{14}C cycle can vary (i.e. ^{14}C as $^{14}CO_2$ is fixed into the plant matter via photosynthesis with this ^{14}C record reflecting these different growth periods because of the intra-annual variations in ^{14}C levels). Such differences in growing season may relate to spatial variation (different regions of the NH with different climate regions and hence growth periods) or altitude (where this affects growth period (*66*)). For example, the general dry-farming (versus limited instances of irrigation) growing season in the Mediterranean is October to May with harvest then variously in May through July (see below). This is almost the opposite intra-annual period versus the period of wood formation in the NH trees comprising IntCal. Underlying this there is also a small latitude effect for ^{14}C ages in the mid-latitudes (*5–9*). We can refer to the available data from intra-annual sampling in the recent past (*22, 60–64, 67–69*), and approximately exclude the effects of modern fossil fuel contribution (*22, 61, 62, 69*), and atmosphere-biosphere exchange. This leaves the underlying (pre-modern, pre-industrial) seasonal *maximum* intra-annual variation for the mid-latitude NH due to recurrent changing stratosphere-troposphere exchanges in the extra-tropical and sub-polar region as potentially producing variation on the order of up to ≤4‰ (~32 ^{14}C years), and likely in a typical range of around 2 to 3‰ (so ~16 to 24 ^{14}C years). This is the natural NH seasonal variability between early spring minima and late summer maxima. We use the approximate figure of ~3‰ above. In support of such an approximate estimate, the intra-hemispheric location-dependent (regional) differences identified in ref. 14 were of a similar order (~2.5‰), as was the offset determined for pre-modern samples from Egypt (*16, 23*).

Work by a number of groups have reported data sets which indicate instances of likely differences (offsets) in contemporary (same year) terrestrial ^{14}C measurements (*14–18, 70–76*). Some causal mechanisms are specific and regional: for example coastal upwelling influencing the local atmosphere (*70, 71*), or release of stored $^{14}CO_2$ from permafrost (*71–73*). Otherwise, such variations are often associated either with the changing impact of a reservoir (e.g. ocean) on a region over time (*75, 76*), or with temporal differences in the timing of plant growing seasons and hence $^{14}CO_2$ uptake, with effects perhaps maximized under certain conditions (*15–18, 66, 77*). Intra-annual data, and time-series of annual to decadal data, indicate that such offsets appear to vary over time (*15, 18, 74, 77, 78*).

An additional factor for consideration for this topic is the utilization of nonstructural carbon in deciduous trees when they begin their new spring growth. This incorporates previous year(s) stored carbon, and hence the initial early wood could, or should, reflect part of the previous year(s) ^{14}C record (*26*). In a small-scale investigation, the contribution of stored carbon was estimated as between about one-third to less than one-half the seasonal effect, but is thus

nonetheless relevant (either minimizing the seasonal effect, or increasing it, depending on the rate of ^{14}C production in a given inter-annual period) (*26*). While such issues likely are effectively irrelevant when ^{14}C dating and calibration is based on multi-year blocks of wood (with annual variations largely cancelling each other out), this becomes of importance for single-year ^{14}C calibration. Such findings suggest that employing whole annual rings of deciduous tree species, e.g. deciduous oak, is less than ideal to investigate the annual ^{14}C record. Preference should therefore be given either to the use of tree-rings from non-deciduous tree species, or (for deciduous species) use of the late wood only, where no such re-use of stored carbon occurs. However, in this case, it must then be noted that this renders such a late-wood ^{14}C record more strongly a NH summer record (as noted in the main text as regards the IrO latewood record in ref. 13), and so different from plant matter with winter-spring or spring to earlier summer growth periods.

Typical traditional field crop growth periods in the Mediterranean

The general dry-farming pre-modern traditional to ancient growing season for field crops (e.g. cereals) in the lower to medium elevation Mediterranean is broadly October to May (*79, 80*), with ancient authors (our earliest classical source is Hesiod (*81*)) placing the standard sowing period around the time of the setting of the Pleiades, and harvest when the Pleiades rises. (This is overlooking limited instances of irrigation in antiquity: ref. 82 pp.237–257.) Crops like barley, wheat, oats, peas, lentils, and vetch, are primarily sown in the autumn to winter and then harvested in the late spring to earlier summer. This is the major production cycle/period. Farmers of course had to adjust to the challenges of weather and circumstances, and there was for example some (but much less, and less productive) spring sown cereals (*83–85*). Any given standard timings varied also according to the local conditions, accounting for moisture availability, warmth, and elevation. Recent global warming has seen progressive small changes in sowing and harvest dates (*86*), and we may anticipate modest movement of average dates in the past according to major climate fluctuations. The typical traditional harvest dates (and so the *end* of the growth period) thus vary across the Mediterranean region according to latitude and elevation. Harvest therefore occurs earlier in lower elevation and especially southern areas, e.g. April–May in Jordan, Israel, or May–June in Cyprus and lowland Crete, whereas it is later in northern or higher areas, e.g. for lowland north Greece the harvest is typically from June to early July, and in the mountains of northwest Greece it occurs even later (*85, 87, 88*). In Italy, considering recent traditional practice and Roman evidence, the harvest period for wheat and other cereals is from late spring (warmer areas) and primarily June to July; earlier at lower elevation, and later at higher elevation. In north Africa and southern Spain, cereal harvest (winter wheat and barley) occurs in the warmer, lower areas from May through June, and is later further north and in higher areas (*83, 89–91*). The variations in harvest timings in the Mediterranean would suggest that ^{14}C offsets from the IntCal record related to growing season are likely greatest in areas with earlier overall growing seasons and earlier harvests, i.e., the more southerly, lower elevation, and warmer areas. Some spring-sown Mediterranean crops and tree crops are harvested later (June–August) and offer some partial overlap with the IntCal tree-ring record. Grapes have a later growing period and harvest (end summer to autumn) more parallel with the IntCal tree-ring record. Olive fruits only start to form in later spring/early summer and are harvested much later, from later autumn through winter, moving this crop back at least partly out of kilter versus the IntCal tree-ring record (*83, 85, 87–90*).

Radiocarbon dates and tree-ring samples employed in this study

The Heidelberg (Hd) ^{14}C data on tree-ring samples were obtained, processed and measured as described in previous publications (*15, 24, 27, 38, 77, 92*) employing the Heidelberg low level gas proportional counting (LLGPC) facility. We observe that in the middle of the period (2007) that

the GeO samples reported in ref. 38 were measured that the Hd laboratory participated in the SIRI inter-laboratory inter-comparison exercise (*93*). The eight samples measured (VIRI Samples R, L, M, S, O, U, K, P), exhibited an average ~0.15 offset in $\Delta^{14}C‰$ values versus the consensus values from the exercise (Hd minus consensus $\Delta^{14}C‰$ values of respectively: 0.73, -0.75, 1.77, 2.24, -2.31, -1.35, 0.28, 0.58), again suggesting no substantive offset (see main text discussion). The German Oak (GeO) samples come from the Hohenheim GeO tree-ring chronology (*94*). The Irish Oak (IrO) samples come from the Belfast tree-ring chronology (*95*) (raw tree-ring series data available from: http://www.chrono.qub.ac.uk/bennett/dendro_data/dendro.html). These European oak samples, comprising whole annual growth increments, should largely reflect the main standard growing season for European oaks from spring (late April/start May but in some areas including Ireland starting a little earlier) through the entire summer to sometime from late August to mid-September as observed for mature trees through observation and experience (*96*), and via experimental observations on seedlings (*97*). The Gordion *Juniperus* sp. samples (GOR) come from the Gordion tree-ring chronology (*15, 27, 77, 98*). The data employed in this paper are listed in table S1. A study of modern junipers in the central Anatolian region (not far from Gordion) found the main positive growth association with late Autumn to start of winter (December) and later spring (May-June) precipitation and later winter (February) temperature (*99*). In reverse, growth was affected by, and then restricted/ended by, drier and hotter conditions in later spring (May–June onwards) and then especially by summer heat and dry conditions (*99*). Twelve additional Mannheim (MAMS) data on Turkish Pine (TuP) are also included, with these samples processed and run as described for this facility (*44*) with its MICADAS (IonPlus®) accelerator mass spectrometer (AMS) (*100*).

The Groningen (GrM) data on *Quercus* sp. samples from Noceto, Italy (table S1), followed the standard acid-base-acid (ABA) framework and subsequent refinements (*101*). The first acid (HCl, 4% w/vol, 80^{o}C) step is employed to eliminate any geological carbonates that may have penetrated into the materials. The samples are then rinsed to neutrality with ultra-pure water. The second step involves the application of an alkaline solution (NaOH, 1% w/vol, RT) which dissolves any supramolecular polyphenols (mainly humic acids) that may have been absorbed from the soil. After another rinse to neutrality, a second acid step is employed (HCl, 4% w/vol, 80^{o}C) to ensure no atmospheric CO_2 absorbed during the alkaline phase remains in the reaction vessel. The samples are then rinsed to neutrality once more. For the wood samples, an additional aqueous oxidation step is also applied ($NaClO_2$,/H^+, 2.5% w/vol, 80^{o}C) to isolate the holocellulose fraction. This step is also followed by a final rinse to neutrality. The pretreated materials are then thoroughly dried. Approximately 3.5 mg aliquots of the charred seed and charcoal products, known as the reduced carbon fraction, and 5 mg of the holocellulose extracts, are then weighed into individual tin capsules for combustion in an Elemental Analyser (EA, IsotopeCube NCS, Elementar®). The EA is coupled to an Isotope Ratio Mass Spectrometer (IRMS, Isoprime® 100), which allows the $\delta^{13}C$ value of the sample to be measured, and a fully automated cryogenic system that traps the CO_2 liberated on combustion. When the run is complete, the individual reaction vessels are transferred to a graphitisation manifold, where a stoichiometric excess of H_2 gas (1: 2.5) is added, and the CO_2 gas is reduced to graphite over an Fe(s) catalyst. The graphite samples are then pressed into zinc cathodes, and their radiocarbon ratios measured by a MICADAS (IonPlus®) AMS (*100*). The quality of radiocarbon dates at Groningen CIO is assured through the monitoring of subsidiary data relative to acceptance criteria, International Atomic Energy Agency (IAEA) reference and known-age sample measurement, and regular repetition of pretreatments on the same sample. Subsidiary parameters include but are not limited to: sample pretreatment yields, %C on combustion, $\delta^{13}C$ and $\delta^{15}N$ values, and C:N ratios (bone collagen). Known-age standards of each of the main material types are taken through chemical pretreatment. The standards currently utilised include but are not

limited to: the horse bone from the VIRI interlaboratory comparison; the Owen Buddleia modern charcoal standard (Oxford Radiocarbon Accelerator Unit); background wood from Kitzbuhel, Austria; and assorted dendrochronological tree-rings from the Dutch Cultural Heritage Agency.

The University of Georgia (UGAMS) dates measured at the Center for Applied Isotope Studies (CAIS) at the University of Georgia on the OYM samples were processed using the following protocols and standard laboratory procedures (*102*). The samples were pre-treated using the acid/alkali/acid (AAA) method followed by bleaching. Samples were placed in 1N HCl and heated to 80ºC for 1 hour to remove secondary carbonates and acid-soluble compounds; washed with 0.1 M NaOH to remove possible contamination by humic acids; and treated with dilute HCl a second time to remove atmospheric CO_2. The samples were bleached (5% wt/vol $NaClO_2$, pH=3) for 1 hour at 80˚C followed by 24 hours at room temperature, and rinsed 3x in ultra-pure (Milli-Q) water. The samples were dried and prepared for stable isotope and radiocarbon analysis as described below. Since the samples had not achieved a pure white color, the excess sample underwent the bleaching routine a second time (total bleach time ≥ 48 hours) and now exhibited a pure white color. This white sample material was employed for the dates reported here. Following each acid or alkali treatment the samples were washed in deionized water, centrifuged, and decanted. Samples were dried at 60ºC. For AMS analysis, the cleaned samples were combusted at 900°C in evacuated / sealed quartz ampoules in the presence of CuO. The resulting carbon dioxide was cryogenically purified from the other reaction products and catalytically converted to graphite (*103*). Graphite $^{14}C/^{13}C$ ratios were measured using the CAIS 0.5 MeV accelerator mass spectrometer and normalized using the Oxalic Acid I standard (NBS SRM 4990). To correct for isotopic fractionation, the sample $^{13}C/^{12}C$ ratios were measured separately using isotope ratio mass spectrometry (IRMS) and expressed as $\delta^{13}C$ with respect to PDB, with an error of less than 0.1‰. The quoted uncalibrated dates have been given in radiocarbon years B.P. (before AD 1950), calculated using the Libby half-life of 5568 years. The error is quoted as one standard deviation and reflects both statistical and experimental errors. The quality of radiocarbon dates is assured through the monitoring of known-age standards, including Oxalic Acid I (NBS SRM 4990) and wood from the FIRI interlaboratory comparison (FIRI D,F), as well as anthracite background.

The date on an OYM sample from the Tübitak National 1 MV AMS Laboratory was pretreated and dated according to their standard procedures, comprising a modified acid-alkali-acid method, graphisation, and then measurement by AMS with a 1MV NEC Pelletron accelerator (*104*).

The Noceto oak (*Quercus* sp.) samples employed in this study, NOC-12, NOC-14, are secure parts of a larger tree-ring chronology from the wooden materials recovered at the site (*105*) built following standard dendrochronological methods (*106*) using the Tellervo and Corina software and procedures (*107, 108*) (figs. S6-S8). NOC-12 covers relative years 1035-1188 of this chronology, and NOC-14 covers relative years 980-1206 of this chronology. NOC-12 appears to be from the same original source tree as samples NOC-6, NOC-8, NOC-15, NOC-16 and NOC-20, and NOC-14 appears to be from the same original source tree as samples NOC-19 and NOC-21 (fig. S8). As individual samples (NOC-12 v. NOC-14) or as groups (NOC-6, 8, 12, 15, 16, 20 v. NOC-14, 19, 21) there is a secure crossdate (figs. S6, S8). Specific tree-ring samples for ^{14}C dating were dissected with a steel blade under a binocular microscope; the resultant ^{14}C data by tree-rings are listed in table S1.

The OYM-50 sample from Oymaağaç Höyük (or Nerik) (*109*) comprised a cross-section of *Pinus brutia* (or *halepensis* – differentiation is not possible solely from wood anatomical analysis but the site location favors a likely identification as *Pinus brutia*), with in total 77 tree-rings from pith

to last preserved tree-ring (which was likely the ring below bark since it was preserved around the extant circumference – of which just a small part was missing). The ^{14}C dates on this sample are listed in table S1.

The AA BCP (whole annual growth increment) and latewood (only) IrO data were employed as published (*13*). We use the data as presented in ref. 13 table S1. This lists the known calendar dates for the BCP samples as 3649 cal B.P. (1700 BCE) to 3450 cal B.P. (1501 BCE), a 200-year inclusive series, and the known age IrO as from 3615 cal B.P. (1666 BCE) to 3529 cal B.P. (1580 BCE), an 87-year inclusive series. We can compare the single-year AA BCP data as weighted averages for the same years (or all available years where there is incomplete AA BCP coverage due to missing 3454 and 3456 cal B.P. rings) to those years represented by the multi-year Hd GeO segments (table S1) (weighted average where two or more data are from the identical years). This shows a weighted average offset of AA BCP to Hd GeO of 26.5±2.3 ^{14}C years (n=50 comparisons). For the period centered 1596 cal B.P. (1647 BCE) to 3491 cal B.P. (1542 BCE) the offset is larger: 36.4±2.9 ^{14}C years (n=34 comparisons). This offset must reflect either differences in the ^{14}C ages of the samples, or differences between the two laboratories, or a combination of these factors. The difference over only 24 available comparisons 3614.5 cal B.P. (1665.5 BCE) to 3529.5 cal B.P. (1580.5 BCE) for AA IrO to the Hd GeO (as above) is 27.3±3.9 ^{14}C years B.P. The AA BCP to Hd GeO offset for this same 3614.5 to 3529.5 cal B.P. interval is 33.2±3.3 ^{14}C years B.P. (thus a ~6 ^{14}C year difference matching the internal AA BCP to AA IrO difference of 6.4±2.0 ^{14}C years). The difference between the (same laboratory) AA BCP to AA IrO datasets of, on average, 6.4±2.0 ^{14}C years suggests that there is a small sample-related difference between BCP and IrO (related to differences in latitude, growing season, elevation, or a combination of these factors). The implication of the above comparisons is that most of the remaining difference between the AA BCP and AA IrO data versus the Hd GeO data, around 20 ^{14}C years of difference overall, and up to ~30 ^{14}C years at some periods, is likely a difference between the two laboratories (methods, instruments). Some of this could be a putative LLGPC to AMS ^{14}C offset (see main text, up to perhaps ≤10 ^{14}C years?). The remainder then is likely an inter-laboratory difference (unless a larger AMS ^{14}C to LLGPC offset is established with further work). There appears to be an unexplained discrepancy in ref. 13 in its Fig. 1 and caption. The IrO are there stated in the caption to Fig.1 to be “Irish oak data (1661–1576 BCE; green)”, this would mean an 85-year inclusive series and placed 5 and 4 years later than the known-ages stated in table S1. Examination of the plot in ref. 13 Fig. 1 (both parts A and B) shows the green symbols (in ref. 13 Fig. 1A) or line and shading (ref. 13 Fig. 1B) for the IrO placed at about 1666-1576 BCE (a 91-year sequence). Thus the plot combines the ref. 13 table S1 date for the start of the series and uses the alternative 1576 BCE end date in the ref. 13 Fig. 1 caption (versus 1580 BCE in ref. 13 table S1). The IrO have somehow acquired extra years. We employ the IrO data and calendar ages as reported in ref. 13 table S1, assuming these are likely the accurate values. We therefore have to express concern over the IrO data as plotted in ref. 13 Fig. 1.

We regard the AA BCP dataset (*13*) as offering a likely maximum adjustment case to the IntCal record in the analysis shown in Fig. 6. The reasons are as follows.
(i) The next iteration of IntCal (IntCal20) will also include nearly all the existing data available in IntCal13 (*4*), in addition to the considerable body of new data now available. Thus, despite the numerical weighting by volume from the new AA data (and other new data), this will nonetheless create some lowering of any overall set mean/best fit.
(ii) The AA IrO data (*13*) are slightly more recent on average (by 6.4±2.0 ^{14}C years) than the AA BCP data. This indicates again that including all other data will likely only lower (even if just slightly) the final IntCal value versus the reported AA BCP record. Hence, we consider the AA BCP record as an indication of a maximum change scenario.

We note that use of the ref. 13 AA BCP dataset makes no substantive change to the GOR wiggle-match placement. For example, modifying the IntCal04 dataset 3649 to 3450 cal B.P. with the BCP dataset (*13*) leads to the same best fit (3686 cal B.P.) for the GOR series as reported in the main text and Fig. 1B.

The Gordion (GOR*) Juniperus* sp. data set has been published previously (*15, 27, 77, 98, 110, 111*). A relevant question is whether the ^{14}C offsets we identify in this paper potentially affect the accuracy of the wiggle-match date placement of the time-series, and hence add a substantive complication when undertaking comparisons. Commonsense would suggest that, were we dealing with the case of a short time-series, then the effect of an offset on part or all of this series could indeed change its placement. However, in contrast, when dealing with a long many-century time-series, then you would anticipate that it is the overall pattern that will determine the placement and the effect of a few periods of modest offsets (in either direction) would be minimal on the overall placement (likely cancelling each other out). To explore and quantify, we can consider an experiment. First, we can take the GOR record and simply remove the data from the positively offset periods identified in Fig. 2 and table S2 and then consider the wiggle-match placement found from the remaining non-, or negatively-, offset data. We consider this reduced set (52 dated elements and 56 ^{14}C dates) against IntCal04 as in the main text and the best fit is placed just -3 years ±2, with e.g. GOR ring 816.5 placed 3646±1 cal B.P. (1697±1 BCE) with the full dataset and 3643±2 cal B.P. (1694±2 BCE) with the reduced dataset excluding the offset periods. Second, we can then consider the reverse, and a wiggle-match just with the positively offset data periods identified in Fig. 2 and table S2 (65 dated elements and 72 ^{14}C dates). Here the wiggle-match best fit against IntCal04 is just +4 years ±2 with e.g. GOR ring 776.5 placed 3686±1 cal B.P. (1737±1 BCE) with the full dataset and 3690±2 cal B.P. (1741±2 BCE) with the reduced dataset only including the offset periods. The conclusion, taking the extreme cases, using data from either just positively offset periods, or non-positively (i.e. no offset or negatively offset) periods, is a very small overall range of possible movement in the date placement for the GOR wiggle-match (a total of ~7 years ±2.8) centered around the date placement employed in the main text. We therefore use the placement from the complete dataset (with both positive and non-positive offset periods, which are relatively balanced) and regard the combined placement as likely accurate within very small margins.

OxCal Models, Coding and Weighted Averages

The OxCal software was employed for ^{14}C calibration (*59, 112*) and wiggle-matching analysis (*39*). Version 4.3.2 was employed, except for the Fig. 4A analysis which employed version 4.1.7 as did the re-runs of the ref. 23 model mentioned in the main text. Curve resolution of 1 year was employed. For the wiggle-matches the SSimple outlier model was applied to individual data (*113*). Where more than one ^{14}C date was available on identical material we considered a weighted average value (*114*). Within uses of OxCal we employed the R_Combine function to calculate such weighted averages; otherwise we calculated them following ref. 114 (denoted as wAV). For outlier assessment of the data in an R_Combine and the R_Combine product we used the SSimple Outlier model for the individual data and the SSimple Outlier model (*113*) for the R_Combine itself (following the coding examples in ref. 115).

Climate Change, History and Archaeology at the end of the Late Bronze Age

The end of the Late Bronze Age and the period from then through the earlier Iron Age (12th–10th centuries BCE) is a period of major social, political and economic transformation in the Mediterranean (*53, 116–118*, ref. 119 pp.445-523, ref. 120 pp.129-181, *121*). A number of the long-established major empires and states of the region during the mid to later Late Bronze Age

(~1500–1200 BCE) either collapse, or transform, in substantive ways. The second millennium BCE trade systems and political structures experience major systemic changes or reorientations. The earlier Iron Age sees the emergence of changed or new, mainly smaller, political entities. Among other considerations in discussions of causes and associations, climate changes or perturbations have been linked with this period of transformation (*52, 53, 118, 122–126*).

The Santorini/Thera olive branch

The main text discusses the calendar dating of the last (outermost) ^{14}C-dated section of the published Santorini olive branch sample (*13, 54, 56, 58, 127, 128*). A separate question is whether this date reflects the approximate time of the Thera/Santorini volcanic eruption (on the topic of the date of the eruption, see below). Although the date for the outermost dated segment of the olive branch corresponds well with ^{14}C dates on short-lived (annual) samples from the volcanic destruction level on Thera/Santorini (*54–56, 129*), there has been some debate around this sample and its dating (*130–132,* ref. 133 at pp. 74–79, 175–181, 197–198). Dating of modern olive wood sections illustrates that wood from different locations around the outer circumference of olive tree branches or stems can exhibit varying ages; some were more or less contemporary with the appropriate age range, but other portions yielded ages as much as ~40–50 years older (*132*). We observe, however, that those portions of the olive sections in ref. 132 that visibly are associated with the latest growth regions, or lobes, of the branch/tree stem sections yield the more recent ages. This statement is based on examination of ref. 132 Figs. 2, 3 (in 8 of 9 cases for the tree section and 5 of 5 cases for the branch section). Furthermore, these ages are fairly close to the correct ages: of 2013 CE for the branch (minus the tree growth material between the bark and sampled wood for the ^{14}C date), and the unknown date a few years before 2013 CE for the tree section (Zippori tree, which had been "dead for only a few years before felling in 2013"). Examination of the illustrations of the Santorini olive branch section and the portions sampled for the ^{14}C dates indicates that this represents an ordered sequence of dates out to a growth lobe (ref. 58 Fig. 1, ref. 129 Fig. 5, ref. 134 frontispiece). We note that we accept that ring-counting is not typically possible for olive wood (*130, 131*). Nonetheless, the dating of wood segments from a section of olive wood (stem or branch) progressively from inner to outer segments along a radius offers an ordered time-series (older to more recent) (*54, 56, 128, 133*). Hence there is a reasonable expectation that the date of the outer portion of a growth lobe likely reflects a period not long before the approximate time this branch ceased growing. The hypothesis is that the volcanic eruption killed and buried the branch and parent tree, and the context of the branch find suggests that the tree was alive up until the time of the volcanic eruption which buried it (*58, 127–129*). In turn, the good correspondence of the ^{14}C dates, both on short-lived (annual) plant matter from the volcanic destruction level on Santorini/Thera, and on the olive branch (*54–56, 129*), combined with the find context of the olive branch, with remains of leaves and roots *in situ* (*127–129*), are all consistent with this hypothesis. (And not with suggestions that the branch had been dead for several to many decades before the eruption.)

Dates for the Santorini/Thera eruption

The date estimated for the mid second millennium BCE 'Minoan' Santorini/Thera eruption event in 20th century scholarship up to the 1970s was usually ~1500 BCE (*54–58, 135–138*). This date was derived from interpretations of material and stylistic linkages as recognized archaeologically between the cultures of the Aegean and the east Mediterranean (and especially Egypt, where an approximate historical chronology exists for the mid-later second millennium BCE). If an alternative date was suggested, it was usually to consider a date between 1500 and 1450 BCE. This ~1500 BCE date is the traditional 'low' chronology date (*57, 135*). In contrast, based on radiocarbon dating in particular, as well as discussions considering various possible indications (via ice-cores, tree-rings, speleothems), along with critique and re-assessment of the

archaeological evidence and its interpretation, other scholarship from the 1980s to present has advocated a higher chronology (*54-56, 58, 111, 127–129, 133, 134, 136-140*). This 'high' date places the eruption in the later 17th century BCE, or perhaps in the early 16th century BCE. Not surprisingly, deliberately or unconsciously, there has been something of a push for a compromise (*56, 138,* ref. 141 pp.5-8, *142*). Some 'low' chronology scholarship has suggested dates as early as about 1530/1525 BCE (*143, 144*), and some 'high' chronology scholarship has considered how to close the gap (*56,* ref. 138 pp.12-45, 49-67, 321-340). This might indicate a date around or a little after 1600 BCE (including, for example, possible tree-ring width minima potentially associated with major volcanism 1619-1617 BCE and 1597 BCE (*145*)). The ^{14}C dataset of ref. 13 pushes the field to think in the same direction of a possible compromise, perhaps ~1597 BCE or ~1560 BCE (*13*)—maybe with the eruption associated with the unusual storm events of the Ahmose Stela (*146*)—as does a recent re-assessment of the ice-core and other proxy evidence potentially related with the Santorini eruption (*147*). A date for the Santorini eruption in the early-mid 16th century BCE—thus a little before, or around the start of, the Egyptian New Kingdom, or 18th Dynasty (*23, 49, 133, 138*)—would, nonetheless, require much of the re-thinking of the traditional (low) archaeological synthesis proposed by the 'high' chronology critique (*55-56, 58, 133–142*). In particular, it is important to appreciate that the majority of the long Late Minoan IA period, a high-point of Minoan civilization (the second part of a combined, so-called New Palace, Middle Minoan III–Late Minoan IA acme era), was *before* the Santorini eruption (on the secure basis of stratigraphy). The same applies to the initial Late Bronze Age elsewhere in the Aegean (e.g. Late Helladic I, Late Cycladic I), and contemporary cultural horizons in the east Mediterranean such as the earlier Late Cypriot I period (*54-57, 133-143*). Thus, as with the 'high' chronology, a date for the Santorini eruption around, or a little before, the start of the Egyptian New Kingdom (the 18th Dynasty) places this initial Late Bronze Age cultural horizon contemporary with, and in the context of, the previous and different Hyksos-Levantine world of the east Mediterranean ~1700-1550 BCE. That is before the Egyptian New Kingdom. This is a structural and historically important difference (*138, 148*). However, at the same time, such a compromise early date for the Santorini eruption, somewhere from ~1600 BCE to during the earlier 16th century BCE, would also be much easier to accommodate versus the long-standing general syntheses of the archaeology and history of the eastern Mediterranean. The quote "compromise early chronology", cited in the main text, comes from ref. 138 p.49. As illustrated in Figs. 5 and 6, clarification will come from better definition of the appropriate Mediterranean-relevant ^{14}C record.

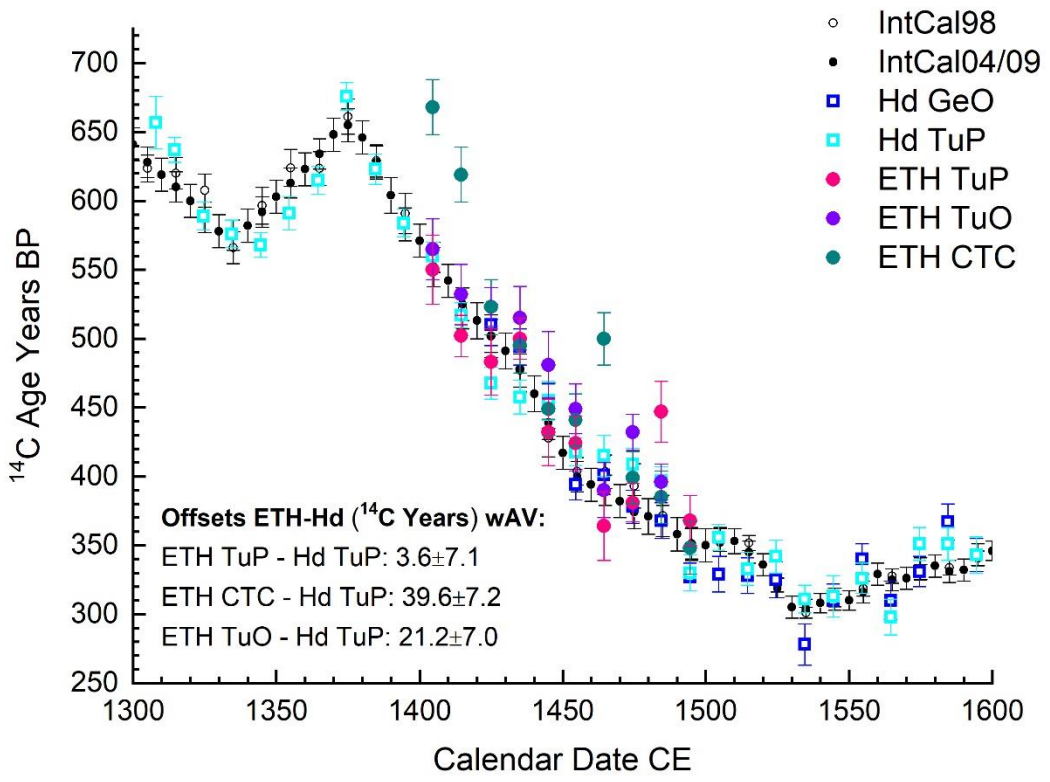

Fig. S1. Comparisons of some ETH AMS ^{14}C data on known-age Mediterranean samples versus Hd data and IntCal98 and IntCal04/09. ETH AMS ^{14}C measurements on known-age Turkish Pine (TuP) from Çatacık, Turkish Oak (TuO) from Bekdemir (*149*), and *Pinus nigra* from the Troodos Mountains in Cyprus (CTC) (*150*) (table S1) versus Hd LLGPC data on similar Turkish Pine (TuP) from Çatacık, Hd data on German Oak (GeO), and versus the IntCal98 and IntCal04/09 calibration datasets (Fig. 1A) (table S1).

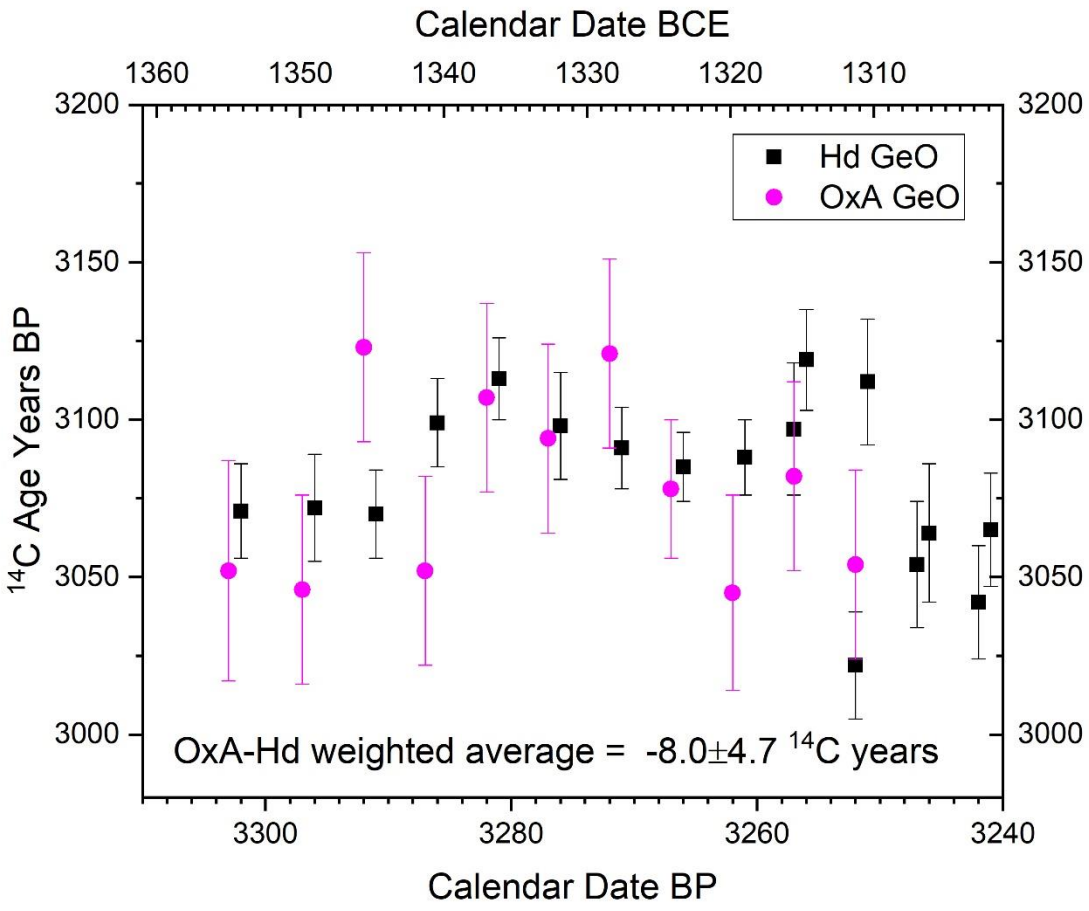

Fig. S2. Comparison of Hd GeO LLGPC measurements (*38*) with OxA AMS ^{14}C measurements on similar GeO (*24*). All error bars 1SD.

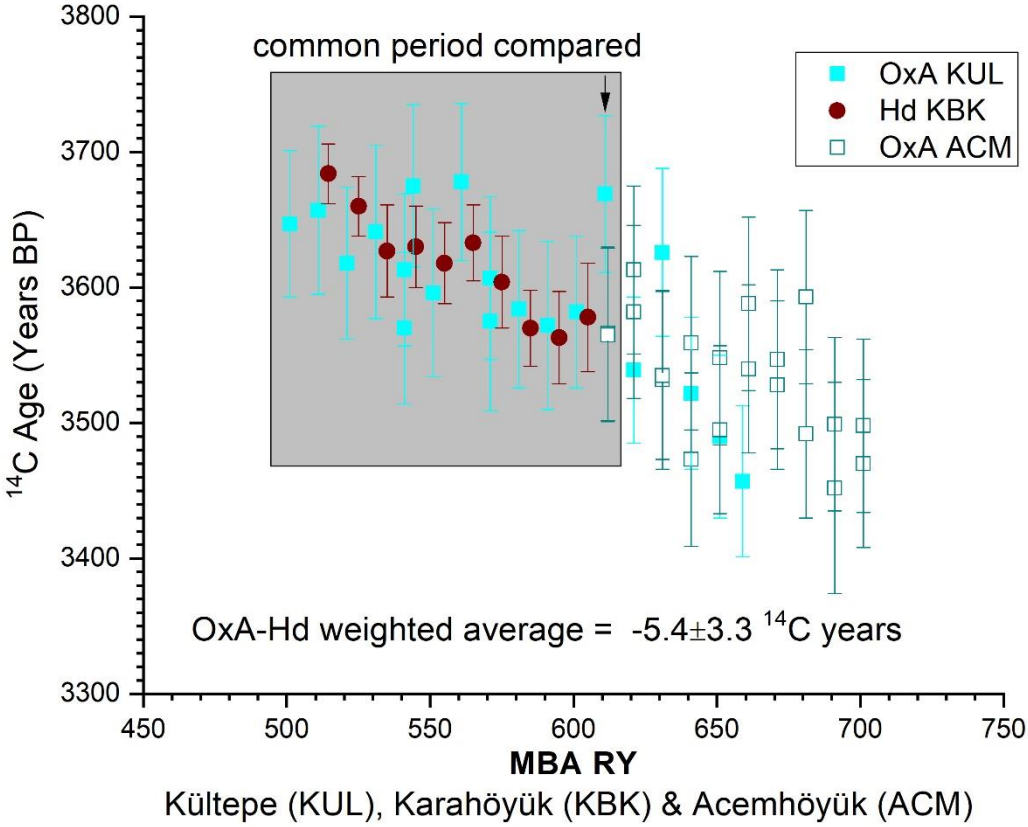

Fig. S3. Comparison of the OxA AMS ^{14}C measurements versus Hd LLGPC measurements on Anatolian juniper samples from a Middle Bronze Age dendrochronological time series built from *Juniperus* sp. samples from the archaeological sites of Kültepe, Acemhöyük, and Karahöyük (*46*). We compare the overlapping datasets at 1-year interpolation, combining the three instances of pairs of OxA data on identical tree-rings. Note: one OxA measurement (OxA-30907), indicated by the arrow, is considered anomalous and an outlier (*46*), and we do not include it in the comparison.

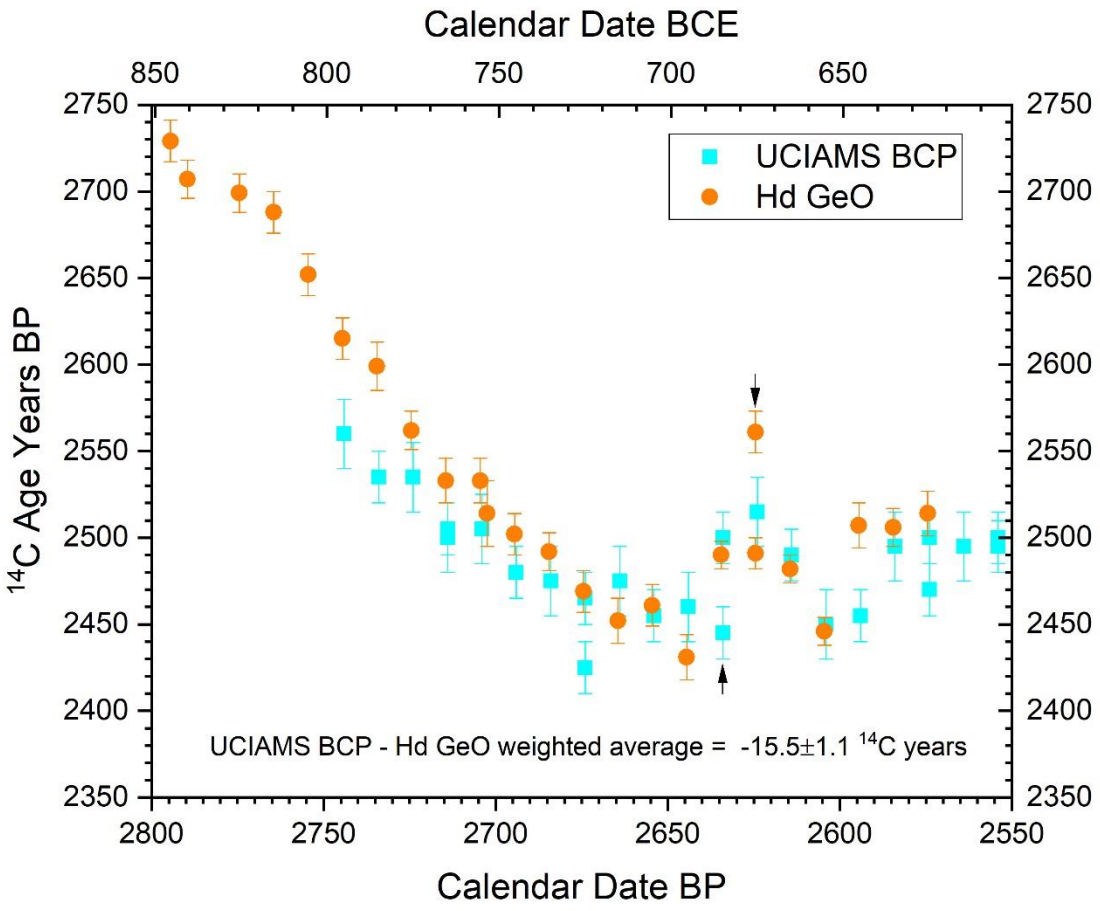

Fig. S4. Comparison of Keck Carbon Cycle Accelerator Mass Spectrometry Laboratory, University of California, Irvine AMS ^{14}C dates on known-age BCP (*40*) versus similar known-age GeO Hd LLGPC ^{14}C data (*38*). All error bars 1SD. The arrows indicate where a pair of UCIAMS data for 2634 cal B.P. and a pair of Hd data for 2624.5 cal B.P. fail a χ^2 test (*114*). Thus rather than employ the weighted average we leave both data in for the comparison between the two series. If the two apparent outlier data (2445±15 ^{14}C years B.P. for UCIAMS and 2561±12 ^{14}C years B.P. for Hd) nearest the two arrows are excluded, then the weighted average difference UCIAMS-Hd becomes -11.4±1.1 ^{14}C years. Note that the UCIAMS BCP values, while similar, are in fact on average slightly more recent than the Hd GeO – in contrast to the older AA BCP values versus same age GeO (Fig. 3A) (*13*).

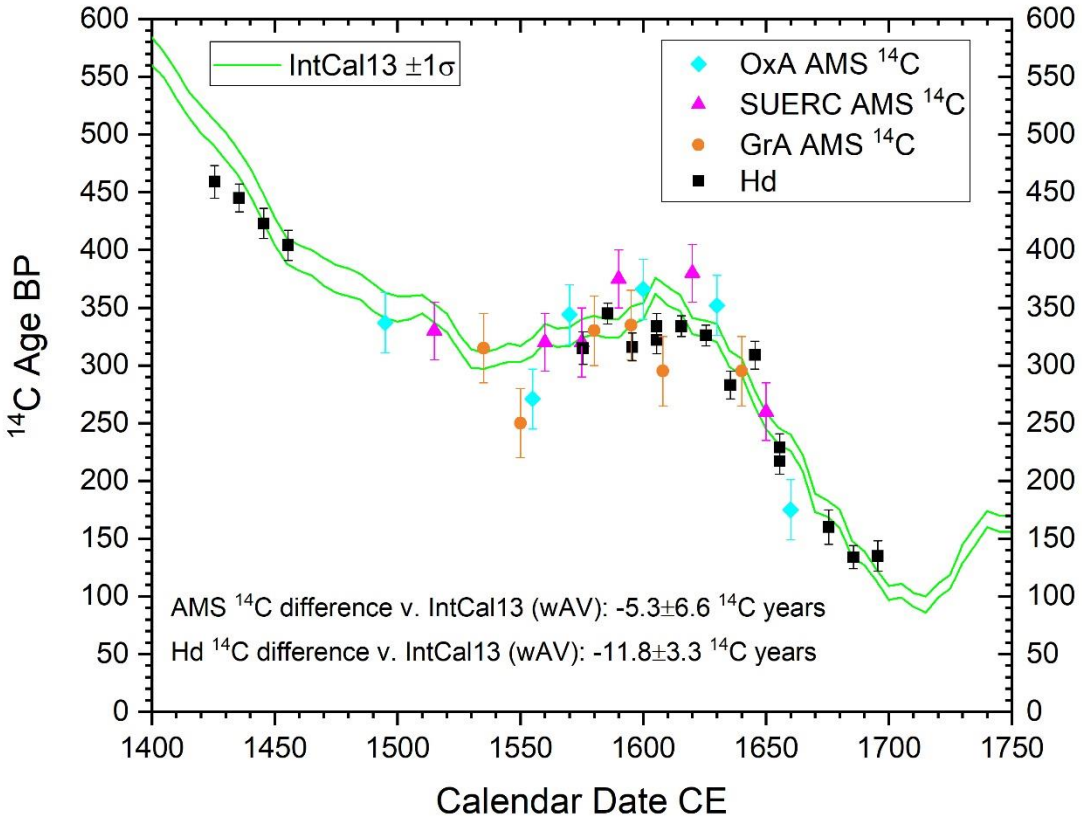

Fig. S5. Comparison of AMS ^{14}C data versus Hd LLGPC ^{14}C ages for similar Swedish pine. AMS ^{14}C measurements from three laboratories (OxA, SUERC, GrA) (*47*) versus Hd LLGPC ^{14}C data all on similar Swedish Pine (*Pinus sylvestris* L.) samples (table S1). Dates on the same tree-rings (same years or same years of Early Wood, EW, and Late Wood, LW) are combined (*114*). The Swedish Pine (*Pinus sylvestris* L.) in ref. 47 comes from a known-age chronology (*151*). The Swedish Pine samples dated at Hd come from central Sweden and were obtained and dendrochronologically dated by Håkan Grudd (for the trees employed, SILJ002, in Siljansfors tree ring set, ULLA001, in Mångberg tree ring set, and HUND001, in Hundtjärn tree ring set, see ref. 152). EW = Early Wood, LW = Late Wood.

	NOC-2 and 9 1034-1192	Averages for crosses with overlaps ≥10: *t*=9.57, *r*=0.57, *tr*=68.1%						
NOC-2 and 9	n=159	NOC-3, 4, and 18 1001-1205						
NOC-3, 4, and 18	t=12.65 r=0.71 tr=72.8%, n=159	n=205	NOC-5 and 17 1009-1202					
NOC-5 and 17	t=7.83 r=0.53 tr=68.4% n=159	t=8.25 r=0.51 tr=68.1% n=194	n=194	NOC-6, 8, 12, 15, 16, and 20 1017-1203				
NOC-6, 8, 12, 15, 16, and 20	t=9.41 r=0.60 tr=70.9% n=159	t=9.11 r=0.56 tr=71.5% n=187	t=10.09 r=0.60 tr=73.0% n=186	n=187	NOC-7 1005-1191			
NOC-7	t=7.87 r=0.53 tr=63.7% n=158	t=8.96 r=0.55 tr=62.4% n=187	t=7.65 r=0.49 tr=60.7% n=183	t=11.97 r=0.67 tr=66.7% n=175	n=187	NOC-10 1001-1198		
NOC-10	t=11.12 r=0.66 tr=69.0% n=159	t=16.87 r=0.77 tr=78.9% n=198	t=7.68 r=0.49 tr=68.0% n=190	t=9.66 r=0.58 tr=64.1% n=182	t=8.72 r=0.54 tr=66.1% n=187	n=198	NOC-11 1022-1200	
NOC-11	t=6.41 r=0.46 tr=62.7%, n=159	t=6.71 r=0.45 tr=61.2% n=179	t=7.03 r=0.47 tr=61.2% n=179	t=9.62 r=0.59 tr=67.4% n=179	t=7.40 r=0.50 tr=59.2% n=170	t=6.37 r=0.43 tr=58.0% n=177	n=179	NOC-14, 19, and 21 1001-1204
NOC-14, 19, and 21	t=7.96 r=0.54 tr=71.5% n=159	t=9.88 r=57 tr=71.7% n=204	t=16.22 r=0.76 tr=81.1% n=194	t=12.45 r=0.68 tr=73.1% n=187	t=8.14 r=0.51 tr=62.9% n=187	t=8.80 r=0.53 tr=67.0% n=198	t=7.90 r=0.51 tr=65.2% n=179	n=204
NOC-22	t=7.48 r=0.51 tr=65.8% n=159	t=9.55 r=0.56 tr=75.7% n=205	t=9.06 r=0.55 tr=69.2% n=194	t=14.70 r=0.73 tr=78.5% n=187	t=9.95 r=0.59 tr=64.5% n=187	t=9.00 r=0.54 tr=71.1% n=198	t=11.06 r=0.64 tr=68.5% n=179	t=10.87 r=0.61 tr=70.9% n=204

Fig. S6. Cross-dating grid for the NOC *Quercus* sp. chronology. Standard dendrochronological methods employed (*106*) with measurements, indexing and crossdating analysis carried out employing Tellervo and Corina software (*107, 108*).

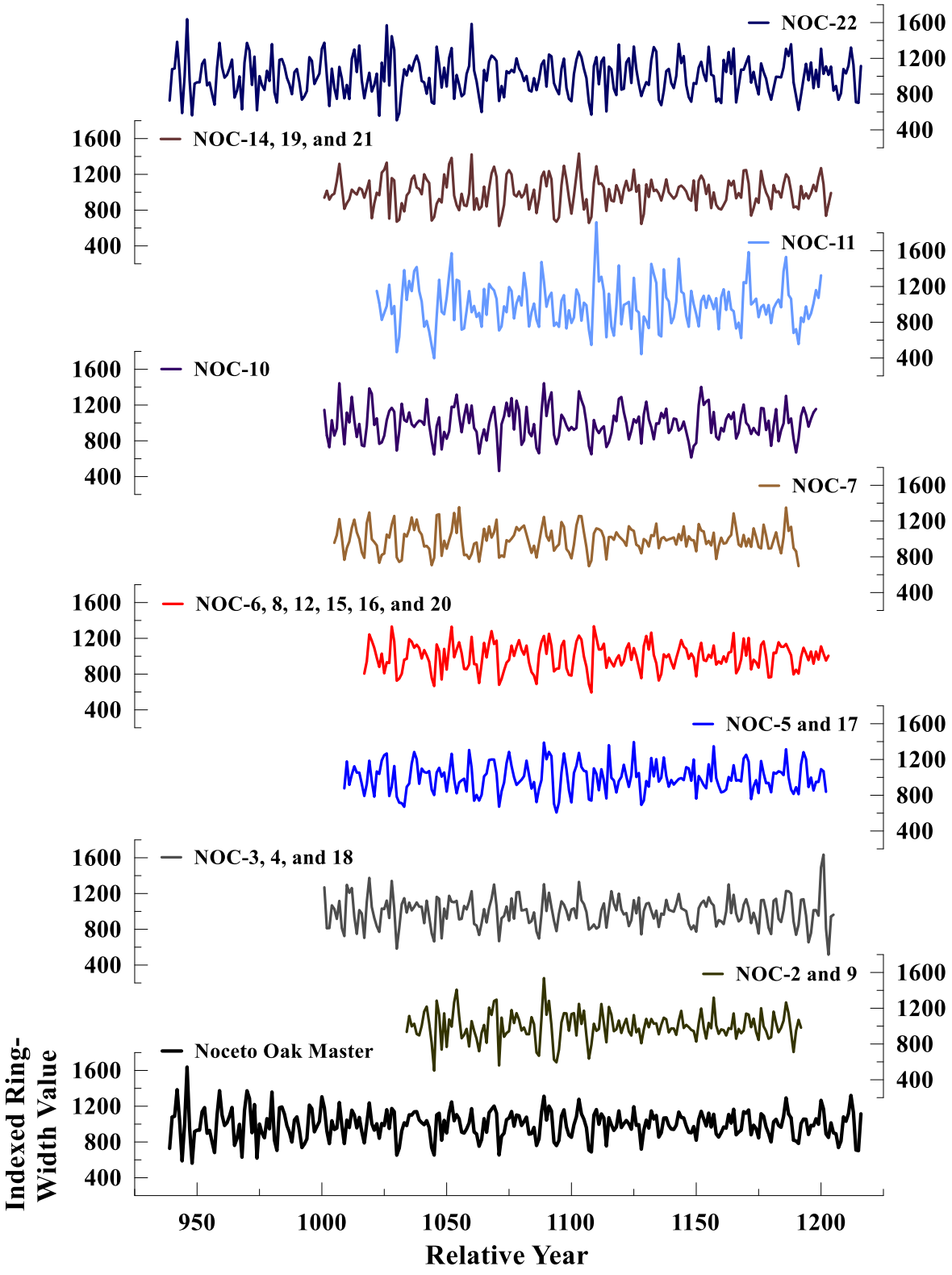

Fig. S7. The indexed tree ring series comprising the NOC *Quercus* sp. chronology.

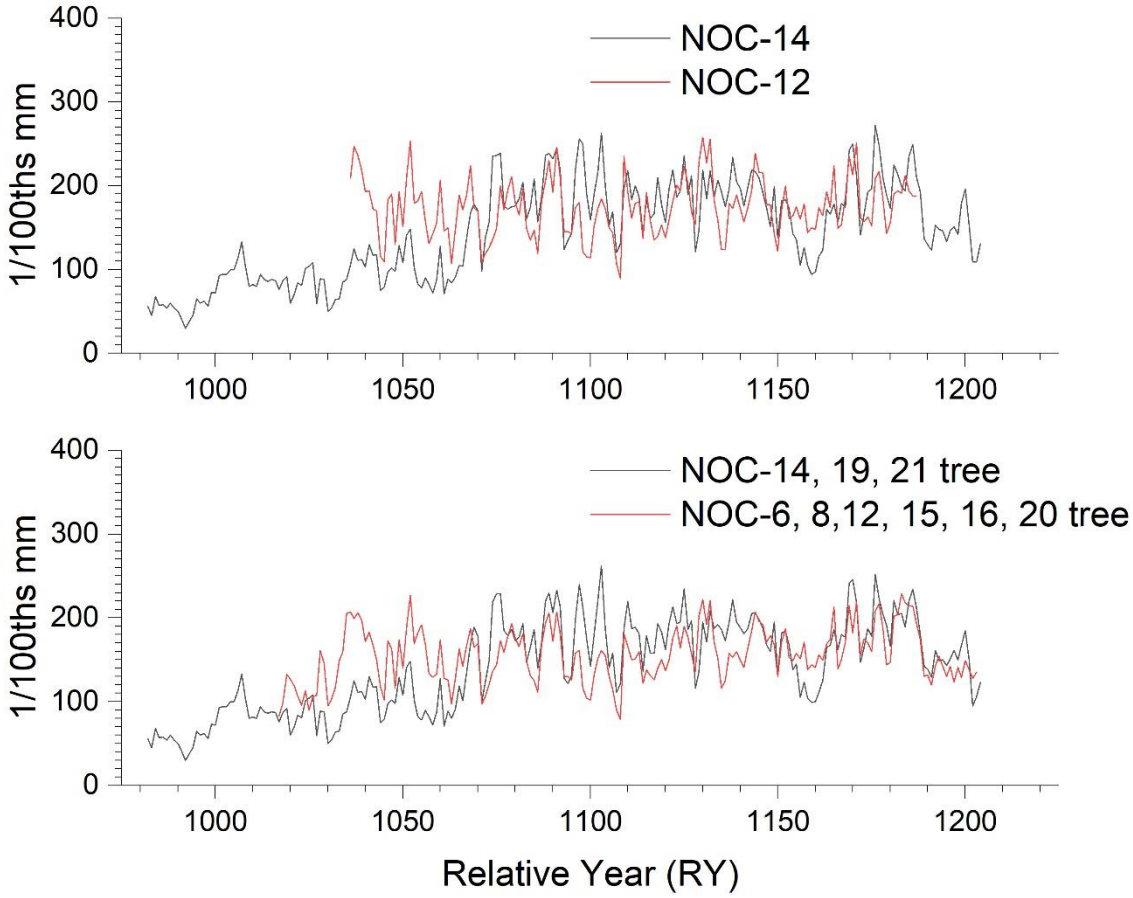

Fig. S8. The tree ring measurements of the NOC-12 and NOC-14 samples within the NOC chronology. We compare the NOC-12 and NOC-14 data individually, and as part of the likely same original source tree groupings that two groups of timbers belong to (NOC-6, 8, 12, 15, 16 and 20, and NOC-14, 19, 21). For the crossdating statistics, see fig. S6.

Table S1. ^{14}C data used in this paper for Figs. 1 to 3 and figs. S1 and S5. The ^{14}C laboratories and ^{14}C date codes are Heidelberg (Hd), Curt-Engelhorn-Centre for Archaeometry, Mannheim (MAMS), Groningen (GrM for dates run on their Micadas AMS and GrA for previous AMS dates), University of Georgia, Center for Applied Isotope Studies (UGAMS), Tübitak MAM Earth and Marine Sciences Accelerated Mass Spectrometry Laboratory (Tübitak), ETH Zürich Laboratory of Ion Beam Physics (ETH), Scottish Universities Environmental Research Centre Radiocarbon Dating Laboratory (SUERC), and Oxford Radiocarbon Accelerator Unit (OxA). If the data have been previously published a reference is provided (otherwise this is the first publication). For samples run on (e.g.) rings 6-11 (6 rings/years) or on 10-year block of tree-rings, e.g. 1400-1409 CE, the mid-point (for plotting and analysis) is treated as the middle, that is between the 8th and 9th, or 5th and 6th, rings respectively for the two examples given. Hence the cal B.P. mid-point is 633.5 for Part 1 date 1 below, or 1404.5 for Part 4 date 1 below, as examples.

***Part 1. Hd and MAMS data on German Oak (GeO), Irish Oak (IrO), Turkish Pine (TuP), Gordion Juniperus* sp.**

cal B.P. Mid	^{14}C B.P.	SD	Lab ID	Rings or Cal Years AD/-BC	Site	Ref
German Oak (GeO) second millennium CE						
633.5	631	13	Hd-23116	6-11	Karlsruhe	110
625.5	586	13	Hd-23117	12-21	Karlsruhe	110
615.5	563	13	Hd-23118	22-31	Karlsruhe	110
605.5	580	13	Hd-23124	32-41	Karlsruhe	110
595.5	600	12	Hd-23125	42-51	Karlsruhe	110
585.5	629	11	Hd-23255	52-61	Karlsruhe	110
575.5	654	13	Hd-23126	62-71	Karlsruhe	110
565.5	642	11	Hd-23035	72-81	Karlsruhe	110
555.5	601	11	Hd-23036	82-91	Karlsruhe	110
545.5	549	10	Hd-23039	92-101	Karlsruhe	110
535.5	515	14	Hd-23119	102-111	Karlsruhe	110
525.5	511	15	Hd-19940	13-22	Creglingen	110
515.5	494	13	Hd-19950	23-32	Creglingen	110
505.5	452	16	Hd-19949	33-42	Creglingen	110
495.5	394	11	Hd-19477	1-10	Aalen	110
485.5	401	14	Hd-19485	11-20	Aalen	110
475.5	378	12	Hd-19484	21-30	Aalen	110
465.5	367	13	Hd-19478	31-40	Aalen	110
455.5	335	10	Hd-19390	41-50	Aalen	110
445.5	331	13	Hd-19440	51-60	Aalen	110
435.5	328	13	Hd-19439	61-70	Aalen	110
425.5	323	14	Hd-19442	71-80	Aalen	110
415.5	278	15	Hd-111816	81-90	Aalen	110
405.5	310	12	Hd-19509	91-100	Aalen	110
395.5	338	11	Hd-19510	101-110	Aalen	110
385.5	310	14	Hd-111815	111-120	Aalen	110
375.5	331	11	Hd-19539	121-130	Aalen	110

365.5	366	14	Hd-111817	131-140	Aalen	110
355.5	341	12	Hd-19548	141-150	Aalen	110
345.5	388	12	Hd-19705	151-160	Aalen	110
335.5	374	13	Hd-19706	161-170	Aalen	110
325.5	371	14	Hd-19737	171-180	Aalen	110
315.5	319	13	Hd-19755	181-190	Aalen	110
305.5	265	12	Hd-19756	191-200	Aalen	110
295.5	243	11	Hd-23056	100-109	Regensburg	110
285.5	211	13	Hd-23057	110-119	Regensburg	110
275.5	151	12	Hd-23055	120-129	Regensburg	110
265.5	155	13	Hd-23059	130-139	Regensburg	110
255.5	131	12	Hd-23073	140-149	Regensburg	110
245.5	92	12	Hd-23072	150-159	Regensburg	110
235.5	100	11	Hd-23051	160-169	Regensburg	110
225.5	150	12	Hd-23048	170-179	Regensburg	110
215.5	172	10	Hd-23047	180-189	Regensburg	110
205.5	180	13	Hd-23061	190-199	Regensburg	110
195.5	180	10	Hd-23053	200-209	Regensburg	110
185.5	168	12	Hd-23054	210-219	Regensburg	110
175.5	205	14	Hd-23062	220-229	Regensburg	110
165.5	189	12	Hd-22883	161-170	Biberach	110
155.5	172	10	Hd-22884	151-160	Biberach	110
145.5	145	10	Hd-22885	141-150	Biberach	110
135.5	119	11	Hd-22886	131-140	Biberach	110
125.5	71	11	Hd-22888	121-130	Biberach	110
115.5	95	10	Hd-22889	111-120	Biberach	110
105.5	105	10	Hd-22890	101-110	Biberach	110
95.5	123	8	Hd-22925	91-100	Biberach	110
85.5	109	10	Hd-22891	81-90	Biberach	110
Irish Oak (IrO) second millennium CE						
85.5	116	9	Hd-23354	1860-1869	Q8513 Slanes Castle	
95.5	99	10	Hd-23427	1850-1859	Q8513 Slanes Castle	
105.5	136	11	Hd-23361	1840-1849	Q8513 Slanes Castle	
115.5	93	11	Hd-23420	1830-1839	Q8513 Slanes Castle	
125.5	97	10	Hd-23417	1820-1829	Q8513 Slanes Castle	
135.5	91	10	Hd-23428	1810-1819	Q8513 Slanes Castle	
145.5	158	10	Hd-23429	1800-1809	Q8513 Slanes Castle	
155.5	194	10	Hd-23416	1790-1799	Q8513 Slanes Castle	
165.5	203	9	Hd-23437	1780-1789	Q8513 Slanes Castle	
175.5	170	11	Hd-23415	1770-1779	Q8513 Slanes Castle	
185.5	182	11	Hd-23356	1760-1769	Q8513 Slanes Castle	
195.5	167	11	Hd-23409	1750-1759	Q8513 Slanes Castle	

205.5	205	9	Hd-23360	1740-1749	Q8513 Slanes Castle	
215.5	153	9	Hd-23469	1730-1739	Q10374 Belvoi Park Forest	
225.5	127	9	Hd-23467	1720-1729	Q10374 Belvoi Park Forest	
235.5	82	11	Hd-23473	1710-1719	Q10374 Belvoi Park Forest	
245.5	112	10	Hd-23447	1700-1709	Q10374 Belvoi Park Forest	
255.5	120	9	Hd-23445	1690-1699	Q1030 Gloverstown House Co. Antrim	
265.5	128	12	Hd-23476	1680-1689	Q1030 Gloverstown House Co. Antrim	
275.5	162	10	Hd-23465	1670-1679	Q1030 Gloverstown House Co. Antrim	
285.5	191	10	Hd-23452	1660-1669	Q10053 Dan Winter's House	
295.5	237	10	Hd-23449	1650-1659	Q10053 Dan Winter's House	
305.5	254	10	Hd-23451	1640-1649	Q10053 Dan Winter's House	
315.5	308	11	Hd-23446	1630-1639	Q10053 Dan Winter's House	
325.5	325	10	Hd-23468	1620-1629	Q10053 Dan Winter's House	
335.5	352	10	Hd-23440	1610-1619	Q934 Pottage House, Co. Antrim	
345.5	358	10	Hd-23453	1600-1609	Q934 Pottage House, Co. Antrim	
Turkish Pine (TuP) second millennium CE						
645.5	651	10	Hd-22611	1309-1300	CAT-1	27
642	657	19	Hd-22810	1309-1307	CAT-1	27
635.5	637	9	Hd-22618	1319-1310	CAT-1	27
625.5	589	10	Hd-22619	1329-1320	CAT-1	27
615.5	576	10	Hd-22620	1339-1330	CAT-1	27
605.5	568	9	Hd-22621	1349-1340	CAT-1	27
595.5	591	12	Hd-22622	1359-1350	CAT-1	27
585.5	615	10	Hd-22623	1369-1360	CAT-1	27
575.5	676	10	Hd-22648	1379-1370	CAT-1	27
565.5	623	11	Hd-22650	1389-1380	CAT-1	27
555.5	584	10	Hd-22671	1399-1390	CAT-1	27
545.5	560	10	Hd-22672	1409-1400	CAT-1	27
535.5	517	9	Hd-22673	1419-1410	CAT-1	27
525.5	463	9.1	Hd-21088+19972	1429.5-1420.5	CAT-15 + CAT-1	27
515.5	452	8.8	Hd-20892+19974	1439.5-1430.5	CAT-15 + CAT-1	27
505.5	455	14	Hd-19970	1449.5-1440.5	CAT-1	27
495.5	406	9.2	Hd-21157+19538	1459-1450	CAT-15 + CAT-1	27
485.5	415	15	Hd-19576	1469-1460	CAT-1	27
475.5	404	9.8	Hd-21245+19506	1479-1470	CAT-15 + CAT-1	27
465.5	396	11	Hd-21246+19505	1489-1480	CAT-15 + CAT-1	27
455.5	330	13	Hd-19481	1499-1490	CAT-15 + CAT-1	27
445.5	354	8.1	Hd-21178+19482	1509-1500	CAT-15 + CAT-1	27
435.5	333	12	Hd-19483	1519-1510	CAT-1	27
429.5	331	11	Hd-24695	1526-1515	CAT-15	27
425.5	342	12	Hd-19508	1529-1520	CAT-1	27

415.5	304	8.6	Hd-21243+19499	1539-1530	CAT-15 + CAT-1	27
405.5	313	15	Hd-19537	1549-1540	CAT-1	27
395.5	326	11	Hd-19580	1559-1550	CAT-1	27
385.5	2118	13	Hd-19521	1569-1560	CAT-1	27
375.5	351	12	Hd-19549	1579-1570	CAT-1	27
365.5	351	12	Hd-19583	1589-1580	CAT-1	27
355.5	343	13	Hd-19551	1599-1590	CAT-1	27
345.5	356	10	Hd-21244+19550	1609-1600	CAT-15 + CAT-1	27
335.5	366	15	Hd-19601	1619-1610	CAT-1	27
325.5	342	11	Hd-21349+19586	1629-1620	CAT-15 + CAT-1	27
315.5	289	12	Hd-20982+19563	1639-1630	CAT-15 + CAT-1	27
305.5	246	13	Hd-19597	1649-1640	CAT-1	27
295.5	238	12	Hd-22674	1659-1650	CAT-1	27
285.5	211	11	Hd-22726	1669-1660	CAT-1	27
275.5	170	13	Hd-22723	1679-1670	CAT-1	27
265.5	157	13	Hd-22755	1689-1680	CAT-1	27
255.5	103	12	Hd-22759	1699-1690	CAT-1	27
245.5	128	10	Hd-22783	1709-1700	CAT-1	27
235.5	100	11	Hd-22728	1719-1710	CAT-1	27
225.5	108	12	Hd-22784	1729-1720	CAT-1	27
215.5	147	12	Hd-22785	1739-1730	CAT-1	27
205.5	179	13	Hd-22786	1749-1740	CAT-1	27
195.5	156	14	Hd-22791	1759-1750	CAT-1	27
185.5	177	15	Hd-22753	1769-1760	CAT-1	27
175.5	197	15	Hd-22758	1779-1770	CAT-1	27
165.5	185	17	Hd-22792	1789-1780	CAT-1	27
155.5	196	14	Hd-22797	1799-1790	CAT-1	27
145.5	138	11	Hd-22800	1809-1800	CAT-1	
135.5	86	13	Hd-22801	1819-1810	CAT-1	
135	81	9	Hd-23480	1820-1810	CAT-6	
125.5	71	13	Hd-22807	1829-1820	CAT-1A	
125	87	9	Hd-23411	1830-1820	CAT-6	
115.5	60	13	Hd-22808	1839-1830	CAT-1A	
115.5	72	10	Hd-24458	1839-1830	CAT-1	
115	85	11	Hd-22410	1840-1830	CAT-6	
105.5	87	12	Hd-24463	1849-1840	CAT-1	
105	104	9	Hd-23414	1850-1840	CAT-6	
98	131	17	MAMS-36594	1850-1854	CAT-6	
93	101	17	MAMS-36595	1855-1859	CAT-6	
88	144	17	MAMS-36596	1860-1864	CAT-1	
83	112	18	MAMS-36597	1865-1869	CAT-1	
68	109	18	MAMS-36598	1880-1884	CAT-6	

63	96	17	MAMS-36599	1885-1889	CAT-6	
58	102	17	MAMS-36600	1890-1894	CAT-6	
53	83	17	MAMS-36601	1895-1899	CAT-6	
48	72	17	MAMS-36602	1900-1904	CAT-6	
43	107	17	MAMS-36603	1905-1909	CAT-6	
38	128	17	MAMS-36604	1910-1914	CAT-6	
33	114	17	MAMS-36605	1915-1919	CAT-6	
German Oak (GeO) 3655-3431 B.P. in Fig. 2B						
3654.5	3471	15	Hd-19803	-1710 to -1701	Sand 21	38
3644.5	3408	15	Hd-20053	-1700 to -1691	Sand 21	38
3644.5	3424	13	Hd-22290	-1700 to -1691	Ebensfeld (1) 99	
3634.5	3396	15	Hd-19800	-1690 to -1681	Sand 21	38
3634.5	3376	13	Hd-22219	-1690 to -1681	Ebensfeld (2) 99	
3624.5	3403	16	Hd-20054	-1680 to -1671	Sand 21	38
3624.5	3396	13	Hd-21587	-1680 to -1671	Ebensfeld (3) 99	
3614.5	3386	15	Hd-19804	-1670 to -1661	Sand 21	38
3614.5	3374	20	Hd-21589	-1670 to -1661	Ebensfeld (4) 99	
3614.5	3409	21	Hd-20098	-1670 to -1661	Knetzgau 40	38
3604.5	3385	16	Hd-19811	-1660 to -1651	Knetzgau 40	38
3604.5	3346	14	Hd-21588	-1660 to -1651	Ebensfeld (5) 99	
3596	3358	23	Hd-26629	-1649 to -1645	Unterbrunn 12 A	38
3594.5	3364	15	Hd-20052	-1650 to -1641	Knetzgau 40	38
3591	3369	19	Hd-26628	-1644 to -1640	Unterbrunn 12 A	38
3586	3326	18	Hd-26647	-1639 to -1635	Unterbrunn 12 A	38
3584.5	3368	16	Hd-19858	-1640 to -1631	Knetzgau 40	38
3581	3344	17	Hd-26646	-1634 to -1630	Unterbrunn 12 A	38
3576	3354	15	Hd-26660	-1629 to -1625	Unterbrunn 12 A	38
3574.5	3343	16	Hd-20123	-1630 to -1621	Knetzgau 40	38
3571	3313	15	Hd-26661	-1624 to -1620	Unterbrunn 12 A	38
3566	3325	14	Hd-26665	-1619 to -1615	Unterbrunn 12 A	38
3564.5	3340	17	Hd-20010	-1620 to -1611	Knetzgau 40	38
3561	3296	12	Hd-26666	-1614 to -1610	Unterbrunn 12 A	38
3556	3282	12	Hd-26696	-1609 to -1605	Unterbrunn 12 A	38
3554.5	3279	14	Hd-19997	-1610 to -1601	Knetzgau 40	38
3551	3297	14	Hd-26697	-1604 to -1600	Unterbrunn 12 A	38
3546	3290	13	Hd-26723	-1599 to -1595	Unterbrunn 12 A	38
3544.5	3280	14	Hd-20012	-1600 to -1591	Knetzgau 40	38
3541	3230	19	Hd-26725	-1594 to -1590	Unterbrunn 12 A	38
3541	3271	14	Hd-27057	-1594 to -1590	Unterbrunn 24 B2	38
3536	3273	19	Hd-26727	-1589 to -1585	Unterbrunn 12 A	38
3536	3261	14	Hd-27056	-1589 to -1585	Unterbrunn 24 B2	38
3534.5	3303	15	Hd-20089	-1590 to -1581	Knetzgau 40	38

3531	3293	12	Hd-27052	-1584 to -1580	Unterbrunn 24 B2	38
3529.5	3278	21	Hd-26728	-1584 to -1577	Unterbrunn 12 A	38
3526	3312	16	Hd-27038	-1579 to -1575	Unterbrunn 24 B2	38
3524.5	3300	16	Hd-20000	-1580 to -1571	Knetzgau 40	38
3521	3302	13	Hd-27053	-1574 to -1570	Unterbrunn 24 B2	38
3516	3288	15	Hd-26852	-1569 to -1565	Unterbrunn 24 B2	38
3514.5	3326	16	Hd-20094	-1570 to -1561	Knetzgau 40	38
3511	3286	15	Hd-26853	-1564 to -1560	Unterbrunn 24 B2	38
3506	3283	13	Hd-26839	-1559 to -1555	Unterbrunn 25 B	38
3504.5	3276	16	Hd-20097	-1560 to -1551	Knetzgau 40	38
3501	3311	12	Hd-26840	-1554 to -1550	Unterbrunn 25 B	38
3501	3271	13	Hd-28134	-1554 to -1550	Knetzgau 3	
3496	3263	16	Hd-26809	-1549 to -1545	Unterbrunn 25 B	38
3496	3311	12	Hd-28132	-1549 to -1545	Knetzgau 3	
3494.5	3307	17	Hd-20009	-1550 to -1541	Knetzgau 40	38
3491	3259	15	Hd-26812	-1544 to -1540	Unterbrunn 25 B	38
3491	3269	13	Hd-28131	-1544 to -1540	Knetzgau 3	
3486	3300	15	Hd-26813	-1539 to -1535	Unterbrunn 25 B	38
3486	3288	11	Hd-28130	-1539 to -1535	Knetzgau 3	
3484.5	3297	16	Hd-20102	-1540 to -1531	Knetzgau 40	38
3481	3294	20	Hd-26772	-1534 to -1530	Unterbrunn 25 B	38
3476	3246	12	Hd-26771	-1529 to -1525	Unterbrunn 25 B	38
3474.5	3248	17	Hd-19996	-1530 to -1521	Knetzgau 40	38
3471	3266	14	Hd-26770	-1524 to -1520	Unterbrunn 25 B	38
3466	3262	22	Hd-26763	-1519 to -1515	Unterbrunn 25 B	38
3464.5	3254	14	Hd-20122	-1520 to -1511	Ebensfeld	38
3461	3284	14	Hd-26764	-1514 to -1510	Unterbrunn 25 B	38
3456	3228	16	Hd-26765	-1509 to -1505	Unterbrunn 25 B	38
3454.5	3276	16	Hd-20129	-1510 to -1501	Ebensfeld	38
3451	3208	21	Hd-26739	-1504 to -1500	Unterbrunn 25 B	38
3451	3236	17	Hd-27073	-1504 to -1500	Unterbrunn 3 D	38
3446	3199	13	Hd-27076	-1499 to -1495	Unterbrunn 3 D	38
3444.5	3206	15	Hd-19994	-1500 to -1491	Knetzgau 40	38
3441	3193	13	Hd-27065	-1494 to -1490	Unterbrunn 3 D	38
3436	3183	15	Hd-27066	-1489 to -1485	Unterbrunn 3 D	38
3431	3197	15	Hd-27075	-1484 to -1480	Unterbrunn 3 D	38
Gordion (GOR) data, Relative Years						
776.5	3430	14	Hd- 19793	772-781	GOR- 161	27
786.5	3409	13	Hd- 20171	782-791	GOR- 161	27
796.5	3432	16	Hd- 19799	792-801	GOR- 161	27
806.5	3426	13	Hd- 20160	802-811	GOR- 161	27
816.5	3403	18	Hd- 19983	812-821	GOR- 161	27

826.5	3335	16	Hd- 19993	822-831	GOR- 161	27
836.5	3348	17	Hd- 20163	832-841	GOR- 161	27
846.5	3401	16	Hd- 19969	842-851	GOR- 161	27
856.5	3372	13	Hd- 20158	852-861	GOR- 161	27
866.5	3356	18	Hd- 19982	862-871	GOR- 161	27
876.5	3342	16	Hd- 20250	872-881	GOR- 161	27
886.5	3334	18	Hd- 19984	882-891	GOR- 161	27
896.5	3336	19	Hd- 20251	892-901	GOR- 161	27
906.5	3235	17	Hd- 19990	902-911	GOR- 161	27
906.5	3280	16	Hd- 24489	902-911	GOR- 76	27
916.5	3302	14	Hd- 20252	912-921	GOR- 161	27
916.5	3329	14	Hd- 24487	912-921	GOR- 76	27
925.5	3323	22	Hd- 26027	921-930	GOR- 161	27
926.5	3284	17	Hd- 20134	922-931	GOR- 161	27
926.5	3308	16	Hd- 24488	922-931	GOR- 76	27
935.5	3329	23	Hd- 26028	931-940	GOR- 161	27
936.5	3338	18	Hd- 20137	932-941	GOR- 161	27
936.5	3296	18	Hd- 24256	932-941	GOR- 76	27
945.5	3330	21	Hd- 26051	941-950	GOR- 161	27
946.5	3289	18	Hd- 20135	942-951	GOR- 161	27
946.5	3288	22	Hd- 24258	942-951	GOR- 76	27
956.5	3310	18	Hd- 20136	952-961	GOR- 161	27
956.5	3322	19	Hd- 24257	952-961	GOR- 76	27
966.5	3292	16	Hd- 20253	962-971	GOR- 161	27
966.5	3319	18	Hd- 24366	962-971	GOR- 76	27
976.5	3292	23	Hd- 20623	972-981	GOR- 161	27
986.5	3223	19	Hd- 19973	982-991	GOR- 161	27
1005.5	3257	18	Hd- 26050	1001-1010	GOR- 87	27
1015.5	3218	18	Hd- 26049	1011-1020	GOR- 87	27
1025.5	3203	20	Hd- 26069	1021-1030	GOR- 87	27
1035.5	3210	21	Hd- 26068	1031-1040	GOR- 87	27
1045.5	3202	17	Hd- 26065	1041-1050	GOR- 87	27
1054.5	3160	22	Hd- 25786	1050-1059	GOR- 3	27
1064.5	3195	21	Hd- 25781	1060-1069	GOR- 3	27
1074.5	3157	32	Hd- 25782	1070-1079	GOR- 3	27
1084.5	3124	21	Hd- 25769	1080-1089	GOR- 3	27
1094.5	3134	19	Hd- 25768	1090-1099	GOR- 3	27
1104.5	3050	20	Hd- 25766	1100-1109	GOR- 3	27
1114.5	3072	17	Hd- 25748	1110-1119	GOR- 3	27
1124.5	3046	18	Hd- 25747	1120-1129	GOR- 3	27
1134.5	3074	18	Hd- 25745	1130-1139	GOR- 3	27
1135	3106	18	Hd- 21774	1130-1140	GOR- 3	27

1135	3062	24	Hd- 21711	1130-1140	GOR- 161	27
1144.5	3049	16	Hd- 25723	1140-1149	GOR- 3	27
1145.5	3045	21	Hd- 26097	1141-1150	GOR- 36	27
1155	3140	38	Hd- 21720	1150-1160	GOR- 161	27
1155.5	3046	21	Hd- 26098	1151-1160	GOR- 36	27
1175	3122	18	Hd- 21721	1170-1180	GOR- 161	27
1185	3144	18	Hd- 21722	1180-1190	GOR- 161	27
1194.5	3088	13	Hd- 24558	1190-1199	GOR- 3	27
1195	3060	19	Hd- 21761	1190-1200	GOR- 161	27
1204.5	3055	13	Hd- 24556	1200-1209	GOR- 3	27
1214.5	3090	18	Hd- 24570	1210-1219	GOR- 3	27
1215	3058	25	Hd- 21712	1210-1220	GOR- 161	27
1224.5	2996	17	Hd- 24559	1220-1229	GOR- 3	27
1264.5	3031	20	Hd- 25726	1260-1269	GOR- 3	27
1274.5	2992	18	Hd- 25714	1270-1279	GOR- 3	27
1284.5	3037	23	Hd- 25708	1280-1289	GOR- 3	27
1294.5	3051	21	Hd- 25706	1290-1299	GOR- 3	27
1304.5	2962	20	Hd- 25707	1300-1309	GOR- 3	27
1314.5	2970	18	Hd- 25681	1310-1319	GOR- 3	27
1324.5	2920	18	Hd- 25688	1320-1329	GOR- 3	27
1325	2909	28	Hd- 10439	1320-1330	GOR- 2	27
1334.5	2956	23	Hd- 25689	1330-1339	GOR- 3	27
1335	2929	20	Hd- 10440	1330-1340	GOR- 2	27
1344.5	2937	19	Hd- 25661	1340-1349	GOR- 3	27
1345	2962	20	Hd- 10441	1340-1350	GOR- 2	27
1354.5	2970	19	Hd- 26965	1350-1359	GOR- 3	27
1364.5	2936	20	Hd- 26966	1360-1369	GOR- 3	27
1374.5	2955	14	Hd- 27000	1370-1379	GOR- 3	27
1375	2955	20	Hd- 10460	1370-1380	GOR- 2	27
1385	2946	19	Hd- 18586	1380-1390	GOR- 2	27
1394.5	2948	15	Hd- 27001	1390-1399	GOR- 3	27
1395	2938	23	Hd- 10822	1390-1400	GOR- 2	27
1404.5	2907	17	Hd- 27002	1400-1409	GOR- 3	27
1405	2899	26	Hd- 10823	1400-1410	GOR- 2	27
1414.5	2912	17	Hd- 27005	1410-1419	GOR- 3	27
1415	2918	23	Hd- 18788	1410-1420	GOR- 2	27
1424.5	2929	15	Hd- 27003	1420-1429	GOR- 3	27
1434.5	2935	17	Hd- 27004	1430-1439	GOR- 3	27
1444.5	2871	19	Hd- 27017	1440-1449	GOR- 3	27
1445	2942	21	Hd- 10461	1440-1450	GOR- 2	27
1454.5	2935	16	Hd- 27018	1450-1459	GOR- 3	27
1464.5	2896	15	Hd- 27016	1460-1469	GOR- 3	27

1474.5	2934	14	Hd- 27020	1470-1479	GOR- 3	27
1484.5	2880	15	Hd- 27021	1480-1489	GOR- 3	27
1485	2868	20	Hd- 10473	1480-1490	GOR- 2	27
1495	2899	14	Hd- 20958	1490-1500	GOR- 2	27
1505	2848	13	Hd- 21044	1500-1510	GOR- 2	27
1515	2895	20	Hd- 10480	1510-1520	GOR- 2	27
1525	2800	15	Hd- 21043	1520-1530	GOR- 2	27
1535	2816	20	Hd- 18587	1530-1540	GOR- 2	27
1545	2779	22	Hd- 18863	1540-1550	GOR- 2	27
1555	2811	20	Hd- 10502	1550-1560	GOR- 2	27
1585	2786	20	Hd- 10688	1580-1590	GOR- 2	27
1605	2728	26	Hd- 21083	1600-1610	GOR- 2	27
1624.5	2746	25	Hd- 21377	1620-1629	GOR- 3	27
1625	2777	20	Hd- 10517	1620-1630	GOR- 3	27
1634.5	2748	18	Hd- 21378	1630-1639	GOR- 3	27
1635	2709	13	Hd- 20980	1630-1640	GOR- 2	27
1644.5	2743	18	Hd- 21322	1640-1649	GOR- 3	27
1645	2734	20	Hd- 10518	1640-1650	GOR- 3	27
1655	2746	20	Hd- 10533	1650-1660	GOR- 3	27
1665	2760	25	Hd- 10542	1660-1670	GOR- 3	27
1674.5	2730	16	Hd- 24696	1670-1679	GOR- 3	27
1675	2720	20	Hd- 10687	1670-1680	GOR- 3	27
1684.5	2683	23	Hd- 24699	1680-1689	GOR- 3	27
1685	2744	18	Hd- 24111	1680-1690	GOR- 3	27
1694.5	2712	18	Hd- 24697	1690-1699	GOR- 3	27
1695	2662	13	Hd- 24055	1690-1700	GOR- 3	27
1705	2640	16	Hd- 24075	1700-1710	GOR- 3	27
1714.5	2666	18	Hd- 21374	1710-1719	GOR- 3	27
1715	2616	12	Hd- 24054	1710-1720	GOR- 3	27
1724.5	2589	21	Hd- 21375	1720-1729	GOR- 3	27
1725	2589	17	Hd- 24076	1720-1730	GOR- 3	27
1725	2549	19	Hd- 24708	1720-1730	GOR- 83	27
1734.5	2610	17	Hd- 21320	1730-1739	GOR- 3	27
1735	2543	17	Hd- 24074	1730-1740	GOR- 3	27
1735	2608	19	Hd- 24705	1730-1740	GOR- 83	27
1744.5	2549	21	Hd- 21321	1740-1749	GOR- 3	27
1745	2555	17	Hd- 24077	1740-1750	GOR- 3	27
1745	2502	36	Hd- 24707	1740-1750	GOR- 83	27
1754.5	2530	25	Hd- 21340	1750-1759	GOR- 3	27

Part 2. GrM measurements on the Noceto (NOC)* Quercus *sp. samples employed in Figure 3A.
We note that GrM-11275 from NOC is an unexplained outlier (too old) and is not plotted or used. The NOC-14 RY1160-1164 sample was subsequently re-prepared and re-dated as GrM-17406. We employ this date.

^{14}C B.P.	SD	Lab ID	Rings, Relative Years	Sample
3380	25	GrM-17548	RY995-999	NOC-14
3375	25	GrM-17645	RY1000-1004	NOC-14
3320	25	GrM-11242	RY1050-1054	NOC-12
3274	15	GrM-13697	RY1050-1054	NOC-14
3332	15	GrM-13749	RY1060-1064	NOC-14
3360	25	GrM-11243	RY1080-1084	NOC-12
3332	15	GrM-13750	RY1080-1084	NOC-14
3317	15	GrM-13751	RY1100-1104	NOC-14
3227	14	GrM-11331	RY1120-1124	NOC-12
3282	15	GrM-13696	RY1120-1124	NOC-12
3260	15	GrM-13752	RY1120-1124	NOC-14
3255	25	GrM-17679	RY1120-1124	NOC-14
3263	15	GrM-13754	RY1140-1144	NOC-14
3330	25	GrM-11275*	RY1160-1164	NOC-12
3250	25	GrM-17406	RY1160-1164	NOC-14
3222	15	GrM-13755	RY1180-1184	NOC-14
3160	35	GrM-17737	RY1200-1204	NOC-14

Part 3. ^{14}C measurements on the Oymaağaç Höyük (OYM)* Pinus brutia *samples employed in Figure 3B. We note that two of the x2 bleach samples for OYM are marked with an asterisk (*). These two dates are unexplained outliers (too old) and are not included in the analysis. The dating of these samples was repeated and we use these repeat dates instead.

^{14}C B.P.	SD	Lab ID	Rings, Relative Years	Sample
2747	19	GrM-14314	1011-1015	OYM-50
2737	20	UGAMS-40841 ABA+bleach	1016-1019	OYM-50
2706	22	UGAMS-40841 ABA+bleachx2	1016-1019	OYM-50
2722	20	UGAMS-40842 ABA+bleach	1020-1022	OYM-50
2662	20	UGAMS-40842 ABA+bleach repeat	1020-1022	OYM-50
2854	23	UGAMS-40842 ABA+bleachx2*	1020-1022	OYM-50
2690	20	UGAMS-40842 ABA+bleachx2 repeat	1020-1022	OYM-50
2763	16	GrM-14415	1031-1035	OYM-50
2710	20	UGAMS-40843 ABA+bleach	1036-1040	OYM-50
2675	22	UGAMS-40843 ABA+bleach repeat	1036-1040	OYM-50
2818	22	UGAMS-40843 ABA+bleachx2*	1036-1040	OYM-50
2721	23	UGAMS-40843 ABA+bleachx2 repeat	1036-1040	OYM-50
2670	21	UGAMS-40844 ABA+bleach	1041-1045	OYM-50
2717	21	UGAMS-40844 ABA+bleachx2	1041-1045	OYM-50
2741	20	UGAMS-40845 ABA+bleach	1046-1050	OYM-50
2713	22	UGAMS-40845 ABA+bleachx2	1046-1050	OYM-50
2785	25	GrM-14445	1051-1055	OYM-50
2699	20	UGAMS-40846 ABA+bleach	1056-1060	OYM-50
2748	23	UGAMS-40846 ABA+bleachx2	1056-1060	OYM-50
2738	21	UGAMS-40847 ABA+bleach	1066-1070	OYM-50
2767	23	UGAMS-40847 ABA+bleachx2	1066-1070	OYM-50
2698	21	UGAMS-39453	1071-1075	OYM-50
2722	23	Tübitak-0172	bark	OYM-50

Part 4. Some ETH ^{14}C data on known age Mediterranean wood samples employed in fig. S1.

Mid Year CE	Calendar Years CE	^{14}C Age B.P.	SD	ETH Lab ID
Cyprus Pine (CTC-64)				
1404.5	1400-1409	668	20	ETH-35594
1414.5	1410-1419	619	20	ETH-35595
1425.5	1421-1430	523	20	ETH-35596
1435.5	1431-1440	495	20	ETH-35597
1445.5	1441-1450	449	19	ETH-35598
1454.5	1450-1459	441	19	ETH-35599
1464.5	1460-1469	500	19	ETH-35600
1474.5	1470-1479	399	19	ETH-35601
1484.5	1480-1489	385	19	ETH-35602
1494.5	1490-1499	348	19	ETH-35603
Turkish Oak (TuO, BEK-6)				
1404.5	1400-1409	565	22	ETH-35604
1414.5	1410-1419	532	22	ETH-35605

1425.5	1421-1430	523	14	ETH-35606
1435.5	1431-1440	515	23	ETH-35607
1445.5	1441-1450	481	24	ETH-35608
1454.5	1450-1459	449	18	ETH-35609
1464.5	1460-1469	390	20	ETH-35610
1474.5	1470-1479	432	13	ETH-35611
1484.5	1480-1489	396	13	ETH-35612
Turkish Pine (TuP, CAT-15)				
1404.5	1400-1409	550	25	ETH-35584
1414.5	1410-1419	502	15	ETH-35585
1425.5	1421-1430	483	24	ETH-35586
1435.5	1431-1440	500	15	ETH-35587
1445.5	1441-1450	432	24	ETH-35588
1454.5	1450-1459	424	20	ETH-35589
1464.5	1460-1469	364	25	ETH-25590
1474.5	1470-1479	381	14	ETH-35591
1484.5	1480-1489	447	22	ETH-35592
1494.5	1490-1499	368	18	ETH-35593

Part 5. ^{14}C dates on known-age Swedish Pine samples employed in fig. S5.

Calendar Date CE Year or Mid-Point	**Years Dated**	**Laboratory ID**	**^{14}C Age Years B.P.**	**SD**	**Reference**
1495	1495	OxA-17254	337	26	47
1515	1515	SUERC-14015	330	25	47
1535	1535	GrA-34748	315	30	47
1550	1550	GrA-34751	250	30	47
1555	1555	OxA-17252	271	26	47
1560	1560	SUERC-14027	320	25	47
1570	1570	OxA-17252	344	26	47
1575	1575	SUERC-14016	320	30	47
1580	1580	GrA-34753	330	30	47
1590	1590	SUERC-14020	375	25	47
1595	1595	GrA-34747	335	30	47
1600	1600	OxA-17251	366	26	47
1608	1608	GrA-35286	295	30	47
1620	1620	SUERC-14026	380	25	47
1630	1630	OxA-17250	352	26	47
1640	1640	GrA-34754	295	30	47
1650	1650	SUERC-14019	260	25	47
1660	1660	OxA-17249	175	26	47

1425.5	1421-1430	Hd-24680	459	14	SILJ 2C
1435.5	1431-1440	Hd-24694	445	12	SILJ 2C
1445.5	1441-1450	Hd-24690	423	13	SILJ 2C
1455.5	1451-1460	Hd-24679	404	13	SILJ 2C
1575.5	1571-1580	Hd-24693	315	14	Ulla 1C
1585.5	1581-1590	Hd-24676	345	9	Ulla 1C
1595.5	1591-1600	Hd-24642	316	12	Ulla 1C
1605.5	1601-1610	Hd-24645	322	12	Ulla 1C
1605.5 EW	1601-1610 EW	Hd-24494	341	16	Ulla 1C
1605.5 LW	1601-1610 LW	Hd-24474	328	15	Ulla 1C
1615.5 EW	1611-1620 EW	Hd-24472	324	12	Ulla 1C
1615.5 LW	1611-1620 LW	Hd-24473	342	11	Ulla 1C
1625.5 EW	1621-1630 EW	Hd-24629	335	11	Ulla 1C
1625.5 LW	1621-1630 LW	Hd-24630	310	15	Ulla 1C
1635.5 EW	1631-1640 EW	Hd-24638	284	17	Ulla 1C
1635.5 LW	1631-1640 LW	Hd-24640	283	15	Ulla 1C
1645.5 EW	1641-1650 EW	Hd-24925	318	15	Ulla 1C
1645.5 LW	1641-1650 LW	Hd-24888	298	17	Ulla 1C
1655.5 EW	1651-1660 EW	Hd-24739	219	14	Ulla 1C
1655.5 LW	1651-1660 LW	Hd-24744	215	16	Ulla 1C
1655.5	1651-1660	Hd-24729	229	12	Ulla 1C
1675.5	1671-160	Hd-24647	160	15	HUND 1E
1685.5	1681-1690	Hd-24639	134	10	HUND 1E
1695.5	1691-1700	Hd-24681	135	13	HUND 1E

Table S2. The nine offset periods identified in Fig. 2A. The start and end years cal B.P. and then the start and end years cal BCE for the offset periods are listed. The offset intervals are where ≥95% of years for a ≥20 consecutive year interval show the Hd GOR ^{14}C dataset values as older than the contemporary IntCal04 (*2*) values.

cal B.P. start	cal B.P. end	cal BCE start	Cal BCE end	Weighted average offset	SD
3686	3656	1737	1707	14.1	3.8
3621	3600	1672	1651	18.2	4.1
3550	3517	1601	1568	21.7	3.5
3328	3243	1379	1294	29.9	2.6
3215	3147	1266	1198	31.1	3.0
3080	3023	1131	1074	19.6	3.1
3017	2941	1068	992	27.4	2.4
2820	2785	871	836	12.8	4.1
2755	2708	806	759	18.6	3.1